

Published in final edited form as:

*Nanoscale*. 2014 February 21; 6(4): 2073–2076. doi:10.1039/c3nr05623f.

## Iron Oxide Nanoparticle Encapsulated Diatoms for Magnetic Delivery of Small Molecules to Tumors

Trever Todd<sup>a,b</sup>, Zipeng Zhen<sup>a,b</sup>, Wei Tang<sup>a,b</sup>, Hongmin Chen<sup>a,b</sup>, Geoffrey Wang<sup>a,b</sup>, Yen-Jun Chuang<sup>c</sup>, Kayley Deaton<sup>a,b</sup>, Zhengwei Pan<sup>c</sup>, and Jin Xie<sup>a,b</sup>

<sup>a</sup>Department of Chemistry, University of Georgia, Athens, GA 30602, United States

<sup>b</sup>Bio-Imaging Research Center (BIRC), University of Georgia, Athens, GA 30602, United States

<sup>c</sup>Faculty of Engineering, University of Georgia, Athens, GA 30602, United States

### Abstract

Small molecules can be co-loaded with iron oxide nanoparticles onto diatoms. With an external magnetic field, the diatoms, after systemic administration, can be attracted to tumors. This study suggests a great potential of diatoms as a novel and powerful therapeutic vehicle.

Despite intensive research endeavors, cancer remains one of the leading causes of death in the United States.<sup>1</sup> One primary challenge in cancer therapy is to deliver therapeutics to tumors site-specifically without affecting normal tissues. The advantages offered by nanotechnology provide a great opportunity for addressing the current limitations of chemotherapy. With nanoparticles as carriers, drugs can stay in the circulation for extended periods of time and preferentially egress into tissues at tumor sites where blood vessels are more permeable.<sup>2</sup> This, in conjunction with malfunctioning lymphatic drainage, leads to preferable drug accumulation in tumors, the so-called enhanced permeability and retention (EPR) effect, which has been the dominant tumor targeting mechanism used by contemporary nanotherapeutics.<sup>3, 4</sup> Over the past decade, many types of nanoparticles have been investigated as drug vehicles. Among them, porous silica nanoparticles have attracted much attention for their low toxicity, biodegradability, and easy fabrication.<sup>5–7</sup> With advanced technologies, silica nanoparticles can be prepared with different dimensions, geometries, and controllable pores on the surface for efficient drug loading.<sup>8</sup>

The efficiency of EPR-mediated tumor accumulation is heavily dependent on tumor vasculature permeability.<sup>9, 10</sup> This characteristic, however, varies drastically among tumor origins, stages, organs, and even across the same masses. Underestimation of this heterogeneity often results in failed translation and lower-than-expectation treatment efficacy with nano-therapeutics.<sup>9</sup> There have been efforts to develop “smart” nano-carriers by conjugating a tumor targeting motif onto particles surfaces’. This active targeting approach, though it may improve tumor cell selectivity, does not necessarily increase nanoparticles’ tumor accumulation.<sup>11</sup> Hence, there is an urgent need to develop a means to improve the delivery efficacy.

One promising approach in this context is magnetic delivery. The concept is to tag drug carriers with magnetic nanoparticles, after which the drugs can be summoned preferably to tumors by applying an external magnetic field at the sites. Magnetic modulation of particle movement has proven to be feasible with iron oxide nanoparticle (IONP)-loaded silica nanoparticles in vitro.<sup>12, 13</sup> Using this method for in vivo delivery, however, has met

challenges. Commonly used silica nanoparticles have a size around 50–100 nm, and can load very limited numbers of IONPs. Such light loading leads to weak magnetic attraction, making magnetotaxis insufficient for in vivo delivery, given a complicated biological environment.

Here we tackle this issue by using diatoms as novel silica vehicles. Diatoms are a major group of algae that are encased within a silica shell called a frustule. Intact diatom shells have a length of approximately 10  $\mu\text{m}$  with  $\sim 500$  nm pores orderly populating their structure. With their much larger size, diatoms, as a carrier, can load significantly higher payloads than common silica nanoparticles. This includes encapsulating hundreds of magnetic nanoparticles per diatom,<sup>14</sup> and in doing so, granting the diatom with a superior magnetic response. In this proof-of-concept study, we successfully loaded a large amount of dye molecules as drug mimics onto IONP-tagged diatoms. Using fluorescence imaging and magnetic resonance imaging (MRI), we confirmed, in small animal tumor models, that these diatoms can be attracted to tumors by magnetic guidance (Scheme 1).

For preparation, raw diatoms (100% Food Grade) were first sonicated and repeatedly washed. Filter paper with 8  $\mu\text{m}$  pores was then used to remove small and broken diatoms. Fig. 1a & b are scanning electron microscope (SEM) images of the purified diatom particles. The frustule shell has a thickness of 2  $\mu\text{m}$ , which wraps to form a hollow cylinder, with an opening at one end. Lengths of the diatoms range from 5 to 15  $\mu\text{m}$ .  $\sim 500$  nm pores are orderly distributed across the particle's surface, both on the walls and on the edges.

For magnetic labeling,  $\sim 15$  nm human serum albumin (HSA) coated IONPs were used. The synthesis and surface modification of the IONPs were reported by us previously.<sup>15</sup> Briefly, IONPs were made by thermal decomposition and were coated with a layer of oleic acid/oleylamine. These nanoparticles were surface-exchanged with dopamine in a 2:1  $\text{CHCl}_3$ /DMSO mixture. The resulting, dopamine coated IONPs were dropwisely added to an aqueous solution of HSA, where the proteins were adsorbed onto the particle surface to grant them with good aqueous stability.

These HSA-IONPs were incubated with diatoms in PBS at room temperature for 2 h. As shown in our previous studies, due to multiple amine groups on the surface, HSA-IONPs are partially positively charged, and may interact with negatively charged surfaces (e.g. cell membranes<sup>15</sup>). It is expected that a similar electrostatic interaction can facilitate the binding of IONPs to the external and internal surfaces of diatom particles. At the end of the incubation, the solution was subjected to centrifugation at a moderate speed to enrich diatoms but not free IONPs. The products, IONP-loaded diatoms (IONP-DTMs), were washed by PBS to remove loosely bound IONPs.

IONP-DTMs were visualized by SEM. Many small particles were found on the diatom surface, which are attributed to immobilized IONPs (Fig. S1a, <sup>†</sup>ESI). The successful loading was also confirmed by energy-dispersive X-ray (EDX) spectroscopy (Fig. S1b, <sup>†</sup>ESI), and more convincingly, by inductively coupled plasma (ICP) analysis, revealing a Fe loading rate of  $\sim 8$  wt%. Such heavy loading of IONPs made diatoms very sensitive to magnetic summoning. Fig. 1c shows that when a magnetic bar was applied, IONP-DTMs were immediately attracted to the wall of the vessel. By contrast, individually dispersed HSA-IONPs were much less responsive to the magnetic attraction (Fig. S2, <sup>†</sup>ESI). Due to a high loading capacity, the loading of IONPs does not affect the ability of diatoms to load small molecules. Fig. 1d shows a study where rhodamine B, a red small molecule dye used as a

---

<sup>†</sup>Electronic Supplementary Information (ESI) available: details on experimental methods, SEM analysis of IONP-DTMs and DTMs after incubation in body fluid mimic. See DOI: 10.1039/c000000x/

drug mimic, was co-loaded with HSA-IONPs onto diatoms. The dye, as a payload, was magnetically attracted to the wall using a magnetic bar.

Next, we studied the cytotoxicity of IONP-DTMs with 4T1 murine breast cancer cells by 3-(4,5-dimethylthiazol-2-yl)-2,5-diphenyltetrazolium bromide, or MTT assays. Within the tested concentration range (0–625  $\mu\text{g}/\text{mL}$ , based on the total mass), the cells kept over 80% viability after 24-h an incubation (Fig. 2). This good biocompatibility is not unexpected given that both silica and HSA-IONPs were low-toxic.<sup>16, 17</sup> We also studied the biodegradability of diatoms in a body fluid mimic.<sup>18</sup> After one-week incubation, we found many broken nanostructures, indicating an ongoing degrading process (Fig. S3, †ESI). Given their relatively large size, however, complete degradation takes a longer time.

With the encouraging *in vitro* data, we moved to *in vivo* investigations to evaluate magnetic delivery with IONP-DTMs. To facilitate the particle tracking, we used ZW800, a near-infrared fluorescence dye, as a drug mimic. With near-infrared emission (ex/em: 780/800 nm), the migration and distribution of ZW800 can be traced *in vivo*. The “drug” loading is similar to that with rhodamine B. These IONP and ZW800 dually labeled diatoms were intravenously (*i.v.*) injected into 4T1 tumor xenograft models (1.65 mg/kg). A magnetic bar was attached to the skin of the tumors before the particle injection and was remained there for one hour. In the control group, no magnet was applied. No abnormalities of animals were observed through the diatom injection. After one hour, the magnet was removed and the animal was subjected to T2-weighted MR imaging. Compared to the pre-scan, no significant signal change was observed in the control group, indicating a minimal tumor accumulation. By contrast, a number of black areas appeared in tumors treated with a magnet (Fig. 3). This signal drop in tumors was accredited to accumulation of IONPs that induce hypointensities. The MRI data correlates well with the *in vivo* fluorescence imaging results, finding dramatic difference in tumor uptake after 1 h (Fig. 4). After the imaging, we sacrificed the animals and dissected tumors for *ex vivo* fluorescence imaging. With region-of-interest (ROI) analysis, it is revealed that more than 6.4 times more particles were accumulated in the tumors treated with a magnet, confirming the good efficacy of magnetic modulation.

## Conclusions

We demonstrated that IONP loaded diatoms could be used *in vivo* as magnetic delivery carriers. To our knowledge, this is the first example of the *in vivo* translation of diatoms. Significant improvement of tumor retention was observed when a magnetic field was applied to the tumor sites. This, together with the low toxicity and biodegradability of IONPs and diatoms, suggest the great potential of the technology. With their big size, diatoms are able to hold a broad range of functionalities. This includes loading multiple types of imaging functionalities for multimodality imaging. It is also possible to load a combination of therapeutics onto diatoms for cocktail cancer therapy. In the current investigation, small molecules were loaded onto diatoms through physical adsorption. Similar to common silica nanoparticles, the surface of diatoms can also be modified by organo-functional silanes to allow introduction of functionalities through covalent linkage. The related investigations are underway.<sup>8</sup>

In the present study,  $\sim 10\ \mu\text{m}$  diatoms were used, which provided a good capacity for nanoparticle/molecule loading. This relatively large size, however, caused undesired particle accumulation in the lung, likely from trapped particles in the narrow capillaries (Fig. 4).<sup>19–21</sup> In future studies, it is important to develop size selection strategies to enrich small-sized diatoms, which may afford better pharmacokinetics. Also, the relatively large pore size may cause a rapid release of drugs. This may be improved by introducing activatable stoppers that can block the pores and only be lifted in response to certain stimuli in tumors.

Similar strategies have been applied to mesoporous silica nanoparticles with success.<sup>22, 23</sup>  
The related research is ongoing in our group.

## Supplementary Material

Refer to Web version on PubMed Central for supplementary material.

## Acknowledgments

This work is supported by the National Institutes of Health (5R00CA153772) and the National Science Foundation (CAREER DMR-0955908).

## Notes and references

1. Siegel R, Naishadham D, Jemal A. *CA-Cancer J Clin.* 2012; 62:10–29. [PubMed: 22237781]
2. Brannon-Peppas L, Blanchette JO. *Adv Drug Deliver Rev.* 2012; 64:206–212.
3. Maeda H, Bharate GY, Daruwalla J. *Eur J Pharm Biopharm.* 2009; 71:409–419. [PubMed: 19070661]
4. Fang J, Nakamura H, Maeda H. *Adv Drug Deliver Rev.* 2011; 63:136–151.
5. Barbe C, Bartlett J, Kong LG, Finnie K, Lin HQ, Larkin M, Calleja S, Bush A, Calleja G. *Adv Mater.* 2004; 16:1959–1966.
6. He QJ, Shi JL. *J Mater Chem.* 2011; 21:5845–5855.
7. Lu J, Liang M, Li ZX, Zink JI, Tamanoi F. *Small.* 2010; 6:1794–1805. [PubMed: 20623530]
8. Slowing II, Vivero-Escoto JL, Wu CW, Lin VSY. *Adv Drug Deliver Rev.* 2008; 60:1278–1288.
9. Prabhakar U, Maeda H, Jain RK, Sevic-Muraca EM, Zamboni W, Farokhzad OC, Barry ST, Gabizon A, Grodzinski P, Blakey DC. *Cancer Res.* 2013; 73:2412–2417. [PubMed: 23423979]
10. Maeda H. *Proc Jpn Acad Ser B Phys Biol Sci.* 2012; 88:53–71.
11. Huang X, Peng X, Wang Y, Wang Y, Shin DM, El-Sayed MA, Nie S. *ACS nano.* 2010; 4:5887–5896. [PubMed: 20863096]
12. Lu CW, Hung Y, Hsiao JK, Yao M, Chung TH, Lin YS, Wu SH, Hsu SC, Liu HM, Mou CY, Yang CS, Huang DM, Chen YC. *Nano Lett.* 2007; 7:149–154. [PubMed: 17212455]
13. Yi DK, Selvan ST, Lee SS, Papaefthymiou GC, Kundaliya D, Ying JY. *J Am Chem Soc.* 2005; 127:4990–4991. [PubMed: 15810812]
14. Losic D, Yu Y, Aw MS, Simovic S, Thierry B, Addai-Mensah J. *Chem Comm.* 2010; 46:6323–6325. [PubMed: 20676447]
15. Xie J, Wang J, Niu G, Huang J, Chen K, Li X, Chen X. *Chem Comm.* 46:433–435.
16. Liu TL, Li LL, Teng X, Huang XL, Liu HY, Chen D, Ren J, He JQ, Tang FQ. *Biomaterials.* 2011; 32:1657–1668. [PubMed: 21093905]
17. Quan QM, Xie J, Gao HK, Yang M, Zhang F, Liu G, Lin X, Wang A, Eden HS, Lee S, Zhang GX, Chen XY. *Mol Pharm.* 2011; 8:1669–1676. [PubMed: 21838321]
18. He QJ, Shi JL, Zhu M, Chen Y, Chen F. *Micropor Mesopor Mat.* 2010; 131:314–320.
19. Illum L, Davis SS, Wilson CG, Thomas NW, Frier M, Hardy JG. *Int J Pharm.* 1982; 12:135–146.
20. Delgado A, Soriano I, Sanchez E, Oliva M, Evora C. *Eur J Pharm Biopharm.* 2000; 50:227–236. [PubMed: 10962232]
21. Willmott N, Chen Y, Goldberg J, Mcardle C, Florence AT. *J Pharm Pharmacol.* 1989; 41:433–438. [PubMed: 2570846]
22. Zhu CL, Lu CH, Song XY, Yang HH, Wang XR. *J Am Chem Soc.* 2011; 133:1278–1281. [PubMed: 21214180]
23. Bhattacharyya S, Wang H, Ducheyne P. *Acta Biomater.* 2012; 8:3429–3435. [PubMed: 22688089]

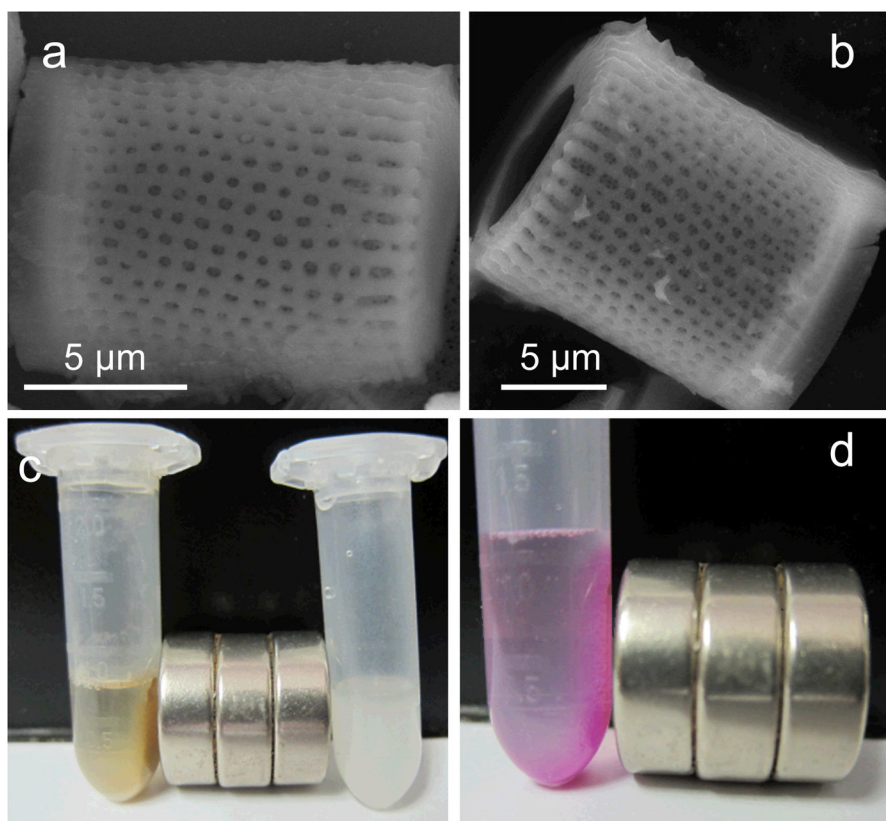


**Figure 1.** (a)&(b) SEM images of diatom particles. (c) Photograph of effect of magnetic field on IONP-DTMs (left) and unloaded diatoms (Right). Without the addition of IONPs, no attraction to the magnet occurs. (d) Rhodamine B can be efficiently onto IONP-DTMs. With the use of a magnet, rhodamine B was attracted to the wall along with the IONP-DTMs.

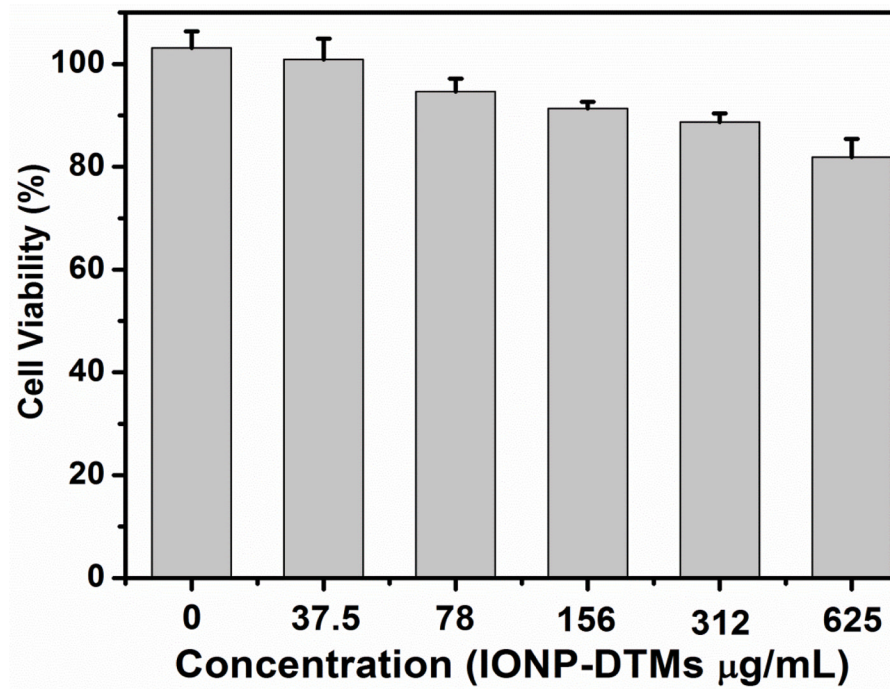


**Figure 2.** Cell viability assay of IONP-DTMs. Cells kept over 80% viability within the tested concentration range (0 – 625  $\mu\text{g/mL}$ ).

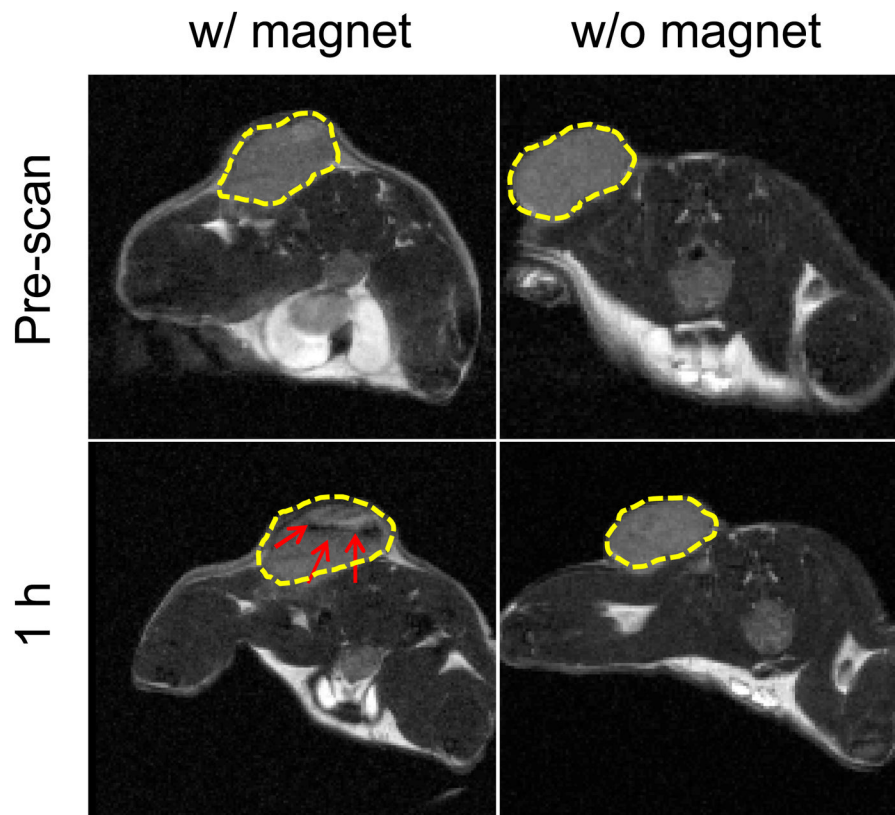


**Figure 3.** T2-weighted MR images taken prior to and 1 h after the injection of ZW800 loaded IONP-DTMs. Black areas (highlighted by red arrows) were observed in tumors where a magnet was attached to the tumor skin. By contrast, no signal change was observed if no magnet was applied.

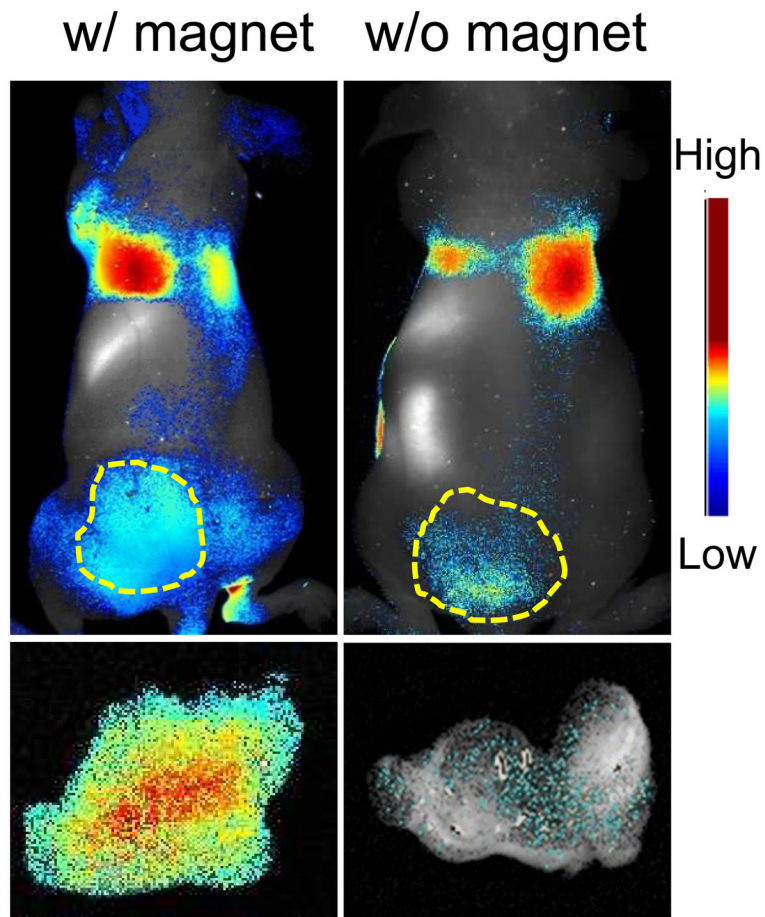
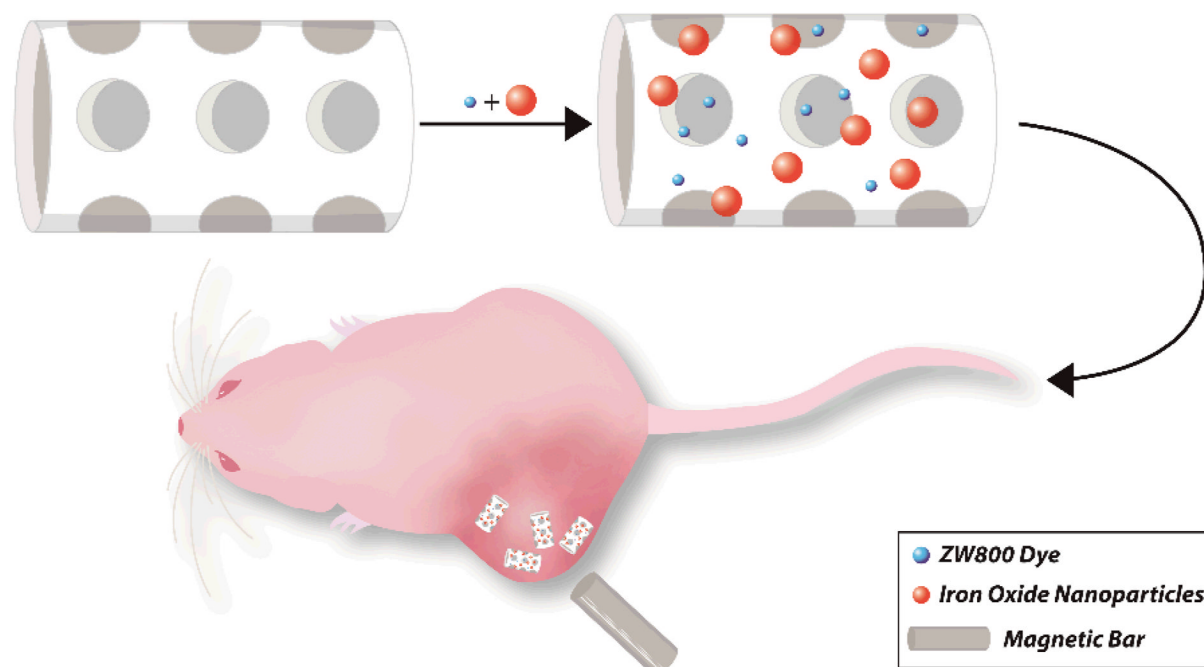


**Figure 4.** (upper row) In vivo imaging results. Correlated to the MRI data, significantly more fluorescence signals were observed in tumors that were attached with a magnet. (bottom row) Ex vivo imaging with dissected tumors. Compared to the controls, 6.4 times higher accumulation of diatoms was observed in the tumors that had been attached with a magnet during the process.



## Magnetic Targeting of IONP Loaded Diatoms



### Scheme 1.

IONP loaded diatoms for magnetic drug delivery. IONPs and small molecule drugs can be loaded into diatom frustules. In response to an external magnet, these diatoms are attracted to tumors after tail vein injection.